ORIGINAL PAPER

Aryl hydrocarbon receptor knock-out exacerbates choroidal neovascularization via multiple pathogenic pathways

Mayur Choudhary,[1] Dmitri Kazmin,[2] Peng Hu,[1] Russell S Thomas,[3] Donald P McDonnell[4] and Goldis Malek[1,5]*

[1] *Department of Ophthalmology, Duke University School of Medicine, Durham, NC, USA*
[2] *Emory Vaccine Center, Emory University, Atlanta, GA, USA*
[3] *Hamner Institutes of Health Sciences, Research Triangle Park, NC, USA*
[4] *Department of Pharmacology and Cancer Biology, Duke University School of Medicine, Durham, NC, USA*
[5] *Department of Pathology, Duke University School of Medicine, Durham, NC, USA*

*Correspondence to: Goldis Malek, Duke University School of Medicine, Departments of Ophthalmology and Pathology, Duke Eye Center, 2351 Erwin Road, AERI Room 4006, Durham, NC 27710, USA. e-mail: gmalek@duke.edu

Abstract

The aryl hydrocarbon receptor (AhR) is a heterodimeric transcriptional regulator with pleiotropic functions in xenobiotic metabolism and detoxification, vascular development and cancer. Herein, we report a previously undescribed role for the AhR signalling pathway in the pathogenesis of the wet, neovascular subtype of age-related macular degeneration (AMD), the leading cause of vision loss in the elderly in the Western world. Comparative analysis of gene expression profiles of aged $AhR^{-/-}$ and wild-type (wt) mice, using high-throughput RNA sequencing, revealed differential modulation of genes belonging to several AMD-related pathogenic pathways, including inflammation, angiogenesis and extracellular matrix regulation. To investigate AhR regulation of these pathways in wet AMD, we experimentally induced choroidal neovascular lesions in $AhR^{-/-}$ mice and found that they measured significantly larger in area and volume compared to age-matched wt mice. Furthermore, these lesions displayed a higher number of ionized calcium-binding adaptor molecule 1-positive (Iba1$^+$) microglial cells and a greater amount of collagen type IV deposition, events also seen in human wet AMD pathology specimens. Consistent with our *in vivo* observations, *AhR* knock-down was sufficient to increase choroidal endothelial cell migration and tube formation *in vitro*. Moreover, *AhR* knock-down caused an increase in collagen type IV production and secretion in both retinal pigment epithelial (RPE) and choroidal endothelial cell cultures, increased expression of angiogenic and inflammatory molecules, including vascular endothelial growth factor A (*VEGFA*) and chemokine (C–C motif) ligand 2 (*CCL2*) in RPE cells, and increased expression of secreted phosphoprotein 1 (*SPP1*) and transforming growth factor-β1 (*TGFβ1*) in choroidal endothelial cells. Collectively, our findings identify AhR as a regulator of multiple pathogenic pathways in experimentally induced choroidal neovascularization, findings that are consistent with a possible role of AhR in wet AMD. The data discussed in this paper have been deposited in NCBI's Gene Expression Omnibus; GEO Submission No. GSE56983, NCBI Tracking System No. 17021116.

© 2014 The Authors. *The Journal of Pathology* published by John Wiley & Sons Ltd on behalf of Pathological Society of Great Britain and Ireland.

Keywords: age-related macular degeneration; aryl hydrocarbon receptor; choroidal neovascularization; RNA sequencing; inflammation; extracellular matrix; angiogenesis

Introduction

Age-related macular degeneration (AMD) is the leading cause of vision loss in the elderly in the Western world [1–3]. The late neovascular subtype, occurring in approximately 10% of patients, is responsible for severe visual impairment and is characterized by the growth of blood vessels from the choroid through Bruch's membrane, resulting in choroidal neovascularization (CNV). The visual decline observed in these patients as a result of CNV can be attributed in part to aberrant neovascularization, vasculogenesis/angiogenesis and, in part, to fibrosis [4–6]. Current treatments target leakage of vessels but are ineffective in treating fibrosis [4,7,8]. Therefore, identification of pathogenic mechanisms involved in all aspects of neovascularization is a critical step in developing more successful therapies. Multiple genetic and environmental risk factors for AMD have been identified to date [9–11], which, independently or in combination, may lead to pathological changes in the structural integrity and function of retinal pigment epithelial (RPE) and choroidal endothelial cells, the cells compromised in CNV formation. Although the specific signalling pathways and biomolecular events which cause cellular dysfunction in AMD are not well understood, RNA transcriptome analysis of eyes from

human AMD donors suggest that diverse pathogenic pathways, including angiogenesis, extracellular matrix (ECM) remodelling, inflammation and the immune response, are perturbed in RPE cells [12,13]. This fact, along with putative crosstalk between RPE cells and the immune and vascular axes, underscores the need to study RPE cells along with other cell types within the microenvironment, eg endothelial cells of the choriocapillaris and choroid, and immune cells including macrophages, when investigating potential pathogenic mechanisms of AMD.

The aryl hydrocarbon receptor (AhR) is a member of the bHLH/PAS (basic helix–loop–helix/Per–Arnt–Sim) family of heterodimeric transcriptional regulators. AhR is important in mediating cellular responses to a wide variety of environmental contaminants, including polycyclic aromatic hydrocarbons, constituents of cigarette smoke and by-products of industrial combustion and automobile exhausts [14–17]. Functionally, AhR has been shown to play a critical role in vascular development, angiogenesis and cancer [18–21], and deficiency in its activity has been linked to peripheral vascular disease, atherosclerosis and tumour development [20–23]. Recently, we found that dysfunction of the *AhR* signalling pathway in aged mice results in pathological features of dry AMD *in vivo* [24]. Moreover, we discovered that the activity of the receptor in human primary RPE cell lines decreases as a function of age, suggesting a potential age-related compromise in normal RPE cellular clearance mechanisms. This is interesting in light of other studies reporting decreased *AhR* expression as a function of age in multiple organs of mice, rats and rabbits [25–27]. Finally, we observed an age-related thinning of the choroidal vascular layers in mice harbouring the *AhR* null allele ($AhR^{-/-}$). These findings, along with the reported regulatory role of AhR in angiogenesis, led us to hypothesize that the *AhR* signalling pathway may regulate pathogenic processes of neovascular AMD. To test this hypothesis, we: (a) investigated the RNA profile of the RPE-choroid of $AhR^{-/-}$ mice; (b) evaluated the severity and morphology of experimentally-induced CNV lesions in $AhR^{-/-}$ mice; (3) examined the effect of *AhR* knock-down on endothelial cell proliferation and migration; and (d) measured the expression of angiogenic, inflammatory and ECM representative genes altered in human CNV, in RPE and choroidal endothelial cell culture models following *AhR* knock-down. The findings support the hypothesis that the AhR plays a role in regulating ECM deposition, immune cell recruitment and angiogenesis, events which constitute necessary steps in the pathogenesis of AMD.

Materials and methods

Animals

Mice used included $AhR^{-/-}$ mice (B6.129-AhR^tm1 Bra/J) [28] originally obtained from Jackson Laboratory (Bar Harbour, ME, USA), where they were bred for 10 generations to C57BL6 mice and an additional two generations to C57BL/6J mice. At Duke University, within the Division of Laboratory Animal Resources, over the last several years they have been bred a minimum of six generations to the 6J background. Additionally, the mice were screened for the confounding retinal degeneration 8 mutation and its absence was confirmed as previously described [24]. Our study protocol was approved by the Duke University Institutional Animal Care and Use Committee. All animal experiments were performed in accordance with the guidelines of the ARVO statement for the Use of Animals in Ophthalmic and Vision Research.

RNA sequencing (RNA–seq) and pathway generation analysis

Mouse RPE-choroid tissue mRNA libraries were prepared using a TruSeq kit (Illumina, San Diego, CA, USA) [29,30]. RPE-choroid pooled from eyes ($n = 2$) was used for each library preparation. Three biological replicate libraries were made from 11–13 month-old $AhR^{-/-}$ and wt mice. Six murine eye libraries were run on two non-independent lanes of the Illumina HiSeq 2500 at the Duke Genome Sequencing and Analysis Core Facility, using 100 bp single-end sequencing. Following quality assessment (FastQC), reads were mapped onto to the University of California Santa Cruz mm10 mouse genome assembly, using TopHat 1.4.0 with Bowtie 0.12.5 alignment engine. Read counts/feature were calculated using HTSeq-count [31], with intersection strict option and using a predefined annotation of known genes from the mm10 genome assembly. Differential transcript abundance was calculated with EdgeR [32,33], utilizing the exactTest procedure. Genes with fewer than one fragments/kilobase of exon/million fragments mapped (FPKM) in more than two samples out of a total of six were not used in differential expression calculations. Significance was defined based on Benjamini–Hochberg false discovery rate (FDR) q values at 0.05 levels. Functional annotation, over-representation analysis and pathway analysis were performed using the GeneGo Metacore pathways software (MetaCore™ v 6.18, build 65505, Thomson Reuters, New York, NY, USA), based on the list of differentially regulated genes produced by EdgeR. False discovery rate was controlled by FDR procedure. The gene ontology (GO) biological process database was used to evaluate functional enrichment.

Mouse model of CNV

Laser photocoagulation was performed in cohorts of young and old wt and $AhR^{-/-}$ mice (4 months old, $n = 8$/genotype; and 11–13 months old, $n = 20$/genotype), as previously described [34]. Briefly, four thermal burns were induced in each eye around the optic nerve, using a slit lamp delivery system. The mice were euthanized 3 weeks after laser treatment and the

eyes were harvested for visualization of laser-induced CNV in posterior pole flat-mounts, or cryopreserved for immunohistochemistry and morphology experiments, as described in Supplementary materials and methods (see supplementary material). CNV lesion volume, area and size were measured in flat-mounts stained with propidium iodide to evaluate cellularity, or isolectin GS-IB$_4$ to examine vascularity, of the neovascular lesion, as described in Supplementary materials and methods.

Cell culture, siRNA transfection and functional assays

Cell lines obtained from ATCC (Manassas, VA, USA) included RF/6A cells, a spontaneously transformed choroidal endothelial cell line derived from the eyes of a rhesus macaque fetus, passages 35–40, and ARPE19 cells, a spontaneously arising human RPE cell line derived from the eyes of a 19 year-old male donor, passages 21–28. Primary cell cultures used included RPE cells (1° RPE) isolated from donor eyes older than 60 years, collected from the North Carolina Organ Donor and Eye Bank Inc. < 6 h post-mortem and cultured within 24 h in accordance with the Declaration of Helsinki for research involving human tissue, as previously described [24]. Small interfering RNAs (siRNAs) were used to knock down *AhR* in cultures of ARPE19, 1° RPE and RF/6A endothelial cells for cell proliferation and viability assays, scrape wound migration assays (MEM 1% CS-FBS), tube formation assays (MEM 1% FBS) and AhR activity assays (7.5% CS-FBS), as described in Supplementary materials and methods (see supplementary material). RNA and protein were extracted at the indicated time points for quantitative real-time PCR (qPCR) and western blot assays. Primer sequences, list of antibodies and dilutions used are provided in Tables S1 and S2 (see supplementary material).

Statistical analysis and data collection

Statistical methods for data analysis other than the RNA-seq experiment included two-tailed Student's *t*-test and two-way ANOVA, with Sidak's multiple comparison test using GraphPad Prism. Values were considered statistically significant at $p < 0.05$. Each *in vitro* experiment was repeated a minimum of three times. Western blots, migration and tube-formation assays shown are representative of a minimum of three independent experiments.

Results

Transcriptomic analysis reveals *AhR* contributions to multiple AMD-related pathways

RNA-seq revealed 392 transcripts differentially expressed between RPE-choroid tissues isolated from aged wt and *AhR*⁻/⁻ mouse eyes. The general distribution of differential gene expression as a function of transcript abundance (M−A plot) is shown in Figure 1A. Annotation performed using MetaCore (Thomson Reuters) pathway software, in conjunction with over-representation analysis of GO terms, highlighted the enrichment of genes in several functional categories (see supplementary material, Table S5). Among these, we focused on GO terms: (a) 'Extracellular matrix organization', GO:0030198 (FDR *p* value 3.137×10^{-6}, 26 of 420 genes present in the list); (b) 'Inflammatory response', GO:0006954 (FDR *p* value 3.577×10^{-6}, 32 of 610 genes); and (c) 'Angiogenesis', GO:0001525 (FDR *p* value 5.757×10^{-4}, 20 of 394 genes). We cross-validated the RNA-seq data from each functional category in *AhR*⁻/⁻ and wt mouse RPE-choroid samples using qPCR (Figure 1B); primers are listed in Table S3 (see supplementary material). We observed down-regulation of *Gpr124*, a regulator of angiogenesis also known as tumour endothelial factor 5 [35,36], down-regulation of the ECM gene collagen type V α1 (*Col5a1*) and up-regulation of the inflammatory gene chemokine (C−C motif) receptor 1 (*Ccr1*) [37,38]. These genes displayed a significant fold change, the direction and magnitude of which was consistent with the RNA-seq analysis.

AhR⁻/⁻ mice develop large CNV lesions compared to age-matched wild-type mice

To determine whether AhR plays a role in the development of CNV, we measured the size, volume and cellularity of laser-induced CNV lesions in flat-mounts of posterior eye cups from 11–13 month-old wt or *AhR*⁻/⁻ mice, stained with propidium iodide (Figure 2A). Larger lesions developed in the eyes of *AhR*⁻/⁻ mice (Figure 2Avii–x) compared to wt (Figure 2Ai–iv), along with a gene-dependent variability in the number of mice with single versus merged lesions (Figure 2B). Specifically, a greater number of *AhR*⁻/⁻ mice presented with three or four merged lesions compared to wt mice (Figure 2Avii–x), which developed at most two merged lesions (Figure 2Aiii, iv). Quantitatively, the mean CNV lesion area was significantly higher in *AhR*⁻/⁻ mice compared with that in wt controls (Figure 2C; normalized to wt, $p < 0.001$). Measurements of CNV lesion thickness and volume determined from *z*-stacks and three-dimensional (3D) reconstruction of images spanning the lesion confirmed a significantly larger lesion volume in *AhR*⁻/⁻ mice versus wt controls. (Figure 2D, E; normalized to wt, $p < 0.0001$, $p < 0.05$; see also supplementary material, Figure S2). Furthermore, vascularity as visualized in flat-mounts stained with isolectin GS-IB$_4$ confirmed an *AhR*-dependent increase in the laser-induced vascular lesion and vessel sprouting (Figure 2Avi, xii). Finally, to determine whether neovascular lesion exacerbation is a result of *AhR* knock-out or a consequence of age, we examined CNV cellularity and vascularity in eyes of 4 month-old *AhR*⁻/⁻ and wt mice ($n = 8$/cohort; Figure 3A) and found a significant increase in lesion
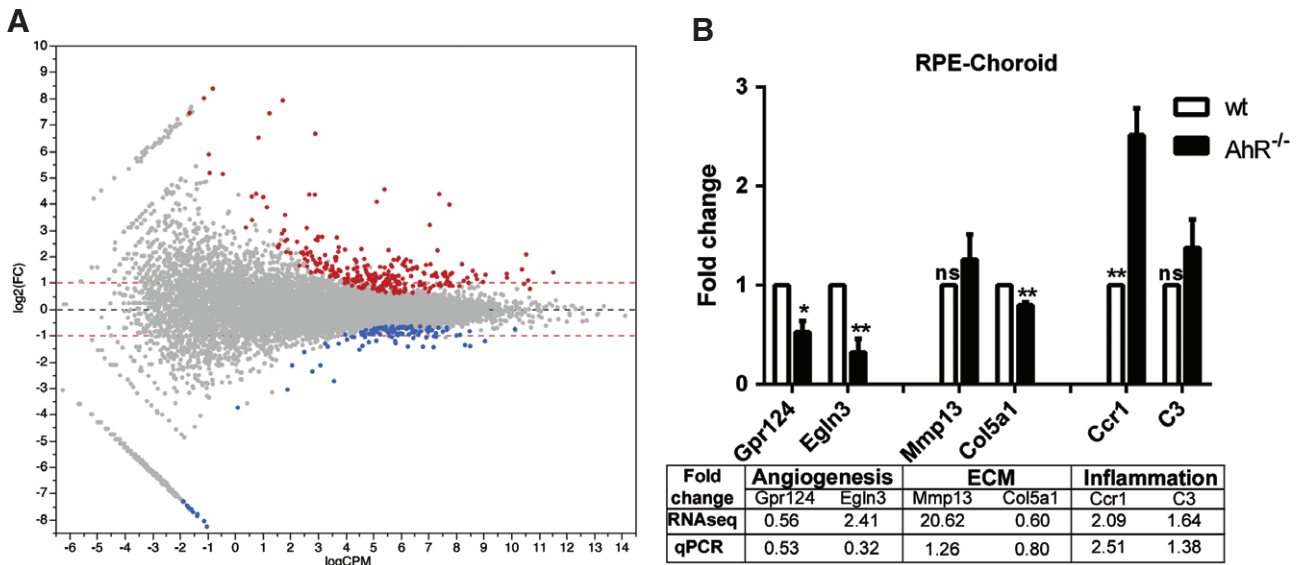
Figure 1. Perturbations of gene expression in RPE-choroid tissue from 11–13 month-old $AhR^{-/-}$ versus wild-type mice. (A) Horizontal axis, log10 of average counts/million (CPM) bases across all samples; vertical axis, log2 of fold change (FC) between knock-out and wild-type animals; each dot represents a feature (gene). Genes regulated at significance level of 0.05 after adjustment for multiple comparisons by FDR are highlighted; up-regulation (red) or repression in knock-out (blue) compared to wild-type. A total of 268 genes are up-regulated in knock-out, while 124 are repressed; red horizontal dashed lines indicate two-fold change level. Among the induced genes, 205 of 268 genes are up-regulated by > 2-fold, while among the repressed genes, 44 of 124 are repressed by > 2-fold; all significantly regulated genes are regulated by > 1.5-fold. (B) qPCR validation of select angiogenic [$Gpr124$ and hypoxia inducible factor 3 ($Egln3$)], extracellular matrix (ECM; $Mmp13$ and $Col5a1$) and inflammatory ($Ccr1$ and $C3$) genes in $AhR^{-/-}$ and wt mouse RPE/choroid samples ($n = 3$/genotype; $^*p < 0.05$, $^{**}p < 0.01$; ns, not significant). Table illustrates fold change as seen by RNA-seq compared to qPCR

area in the knock-out compared to wt mice. (Figure 3B, C). This confirms that the role of *AhR* in CNV lesion formation is due to the absence of a functional gene, rather than being a developmental phenomenon.

AhR signalling pathway is active in ARPE19 and RF6A choroidal endothelial cell lines

Both the RPE and endothelial cells of the choriocapillaries and choroid play a role in CNV formation [8,34]. Previously, we have shown that the AhR signalling pathway is active in human RPE cells [24]. Here, we investigated the AhR signalling pathway in choroidal endothelial cells by determining the expression and activity of the receptor *in vitro*, using RF/6A cells. *AhR* and its obligate binding partner AhR nuclear translocator (*ARNT*) were found to be expressed in both RF/6A cells and excised human choroid specimens (Figure 4A). Following validation of the efficiency of RNA and protein knock-down using three different siAhRs in endothelial cells at 48 and 72 h (Figure 4B, C; see also supplementary material, Figure S3), we assessed AhR transcriptional activity and target gene expression in cells treated with known AhR agonists [2,3,7,8-tetracholorodibenzodioxin (TCDD), benzo(*a*)pyrene (BAP), β-napthoflavone (βNF) and α-napthoflavone (αNF) (see supplementary material, Table S4). AhR agonists activated the receptor in RF/6A cells, while agonist-induced AhR activation was diminished upon receptor knock-down (Figure 4D). Expression of two AhR-specific target genes [cytochrome P450, family 1, subfamily A,

polypeptide 2 (*CYP1A2*) and CYP1, subfamily B, polypeptide 1, (*CYP1B1*)] increased following agonist treatment and once again diminished following knock-down in RF/6A cells (Figure 4E, F; see also supplementary material, Figure S3), supporting the presence of an active AhR signalling pathway in the RF/6A choroidal endothelial cell line.

AhR loss results in increased endothelial migration and tube formation

A key process in neovascularization is cellular organization, which involves endothelial cell migration and sprouting, leading to the formation of an endothelial network [39]. To investigate the effect of *AhR* expression on choroidal endothelial cell migration, a scrape-wound assay was performed on RF/6A cells (Figure 5A). A significantly greater number of cells migrating into the wound were found following knock-down (Figure 5B; $p < 0.0001$). We also determined the effect of *AhR* loss on the ability of endothelial cells to re-organize and form a 3D network, indicative of vascular morphogenesis (Figure 5C). Total tube lengths were significantly longer in cells transfected with siRNAs targeting the *AhR* compared with control (Figure 5D; $p < 0.0001$). Suramin served as an additional control, inhibiting tube formation (Figure 5C). Cell viability and proliferation assays showed no significant differences between siC- and siAhR-transfected RF/6A cells (see supplementary material, Figure S4), or treatment with conditioned media following *AhR* knock-down (see supplementary material, Figure S5), indicating that the increase in
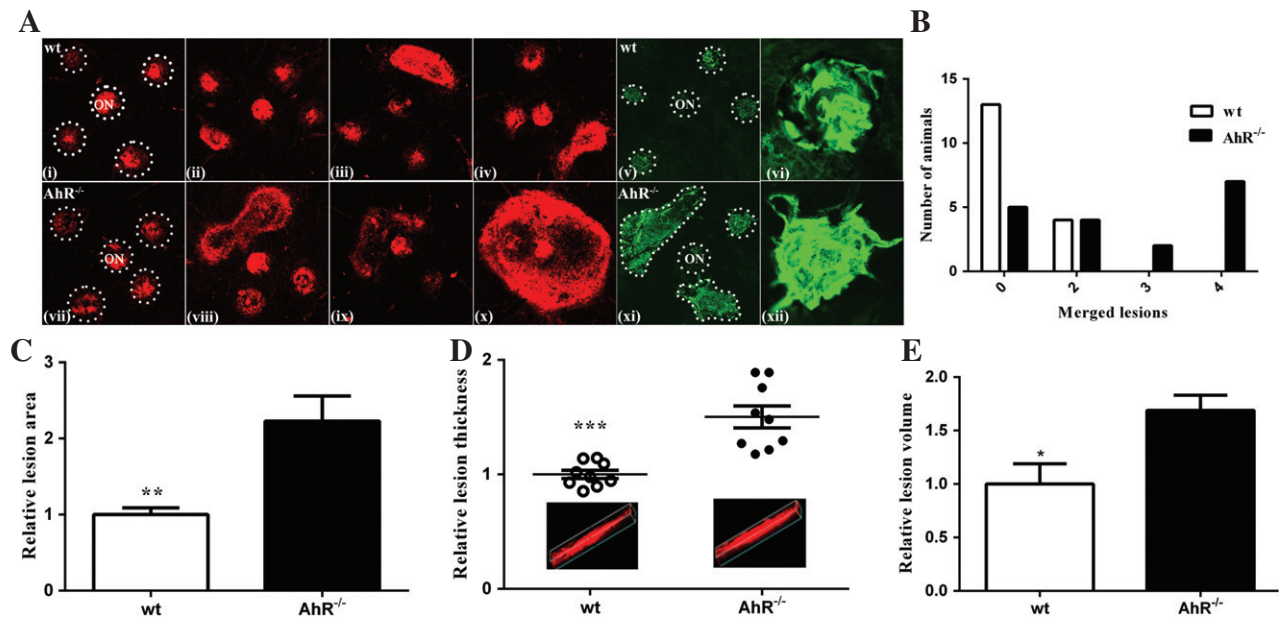
Figure 2. *AhR* regulates laser-induced CNV in aged mice. (A) Choroidal flat-mounts were prepared from 11–13 month-old laser-induced CNV mice (*n* = 20/genotype) and stained with propidium iodide (*AhR*−/−, *AhR* knock-out; ON, optic nerve; i–iv, wt; vii–x, *AhR*−/−; and isolectin GS-IB$_4$, v–vi, wt; xi–xii, *AhR*−/−). Representative images from four eyes/genotype are shown to demonstrate individual and merged CNV lesions (dotted circles demarcate lesions and ON, i and vii) stained with propidium iodide; vi and xii, high-magnification images of individual lesions stained with isolectin GS-IB$_4$. (B) Distribution of number of animals with individual versus merged lesions in wt and *AhR*−/− (*n* = 18/genotype). (C) Relative lesion area/animal was measured using ImageJ (mean and SEM; *n* = 18/genotype; $^{**}p < 0.001$). (D) Relative lesion thickness/animal (mean, SEM and data points for each group; *n* = 9/genotype; $^{***}p < 0.0001$); inserts display representative 3D reconstruction images for wt and *AhR*−/− mice. (E) Relative lesion volume/animal (mean and SEM for each group; *n* = 5/genotype; $^{*}p < 0.05$)

migration and tube formation is not due to a change in cell viability or proliferation. Cumulatively, these results suggest that the loss of *AhR* expression and/or activity may drive endothelial cells towards a pro-angiogenic phenotype.

AhR loss results in increased expression of inflammatory and angiogenic markers

Inflammation has been shown to play a central role in AMD pathogenesis, as activated microglial cells have been detected in the subretinal space of AMD patients [40]. Microglia are normally excluded from the outer retina, due to the presence of immunosuppressive factors secreted by RPE cells [41–44]. In advanced age and following photoreceptor injury, retinal microglia migrate and accumulate within the outer retina [40–42,45] and the neovascular lesion [46]. It is of significance, therefore, that we found an increased number of Iba1+ (Figure 6A) and macrophage chemotactic factor secreted phosphoprotein 1 (SPP1; see supplementary material, Figure S6A)-positive cells within the CNV lesions after laser-induced injury in *AhR*−/− mice compared to wt mice (Figure 6B; see also supplementary material, Figure S6B; *p* < 0.001 and *p* < 0.01). Notably, we have also detected Iba1+ cells subretinally in aged *AhR*−/− in the absence of laser-induced CNV (Figure 6A). Since RPE and choroidal endothelial cells are involved in modulating the microenvironment of the outer retina secondary to the production and secretion of various cytokines and

growth factors, we evaluated the impact of *AhR* loss on the expression of immunomodulatory and inflammatory cytokines/growth factors in ARPE19 and RF/6A cells. A significant increase in expression of chemokine (C–C motif) ligand 2 (*CCL2*) mRNA, important in microglial and macrophage recruitment, and vascular endothelial growth factor A (*VEGFA*) mRNA in ARPE19 cells, was found following *AhR* knock-down (Figure 6C; *AhR* *p* < 0.0001, *VEGFA* *p* < 0.01, *CCL2* *p* < 0.0001). In RF/6A cells we observed an increase in transforming growth factor-β1 (*TGFB1*) mRNA levels, which may contribute to subretinal fibrosis [47], an up-regulation of *SPP1* and down-regulation of the anti-angiogenic factor, *SERPINF1* (Figure 6D; *AhR* *p* < 0.01, *TGFB1* *p* < 0.001, *SPP1* *p* < 0.001, *SERPINF1* *p* < 0.05) [48,49].

AhR loss results in increased expression of collagen

Impaired regulation of ECM turnover is a proposed AMD pathogenic mechanism [4,50]. Further, the ECM molecule, COL4, is a component of sub-RPE deposits and CNV membranes [51,52]. ECM turnover is also regulated in part by AhR in the liver, heart and kidneys [18,53,54]. Recently, we showed that COL4 is a component of the sub-RPE deposits that accumulate in aged *AhR*−/− mouse eyes, and demonstrated increased secretion of this protein from ARPE19 and primary human RPE cells following *AhR* knock-down *in vitro* [24]. With this in mind, and given that sub-RPE deposits, including drusen, are risk factors for the development of CNV, we assessed COL4 deposition
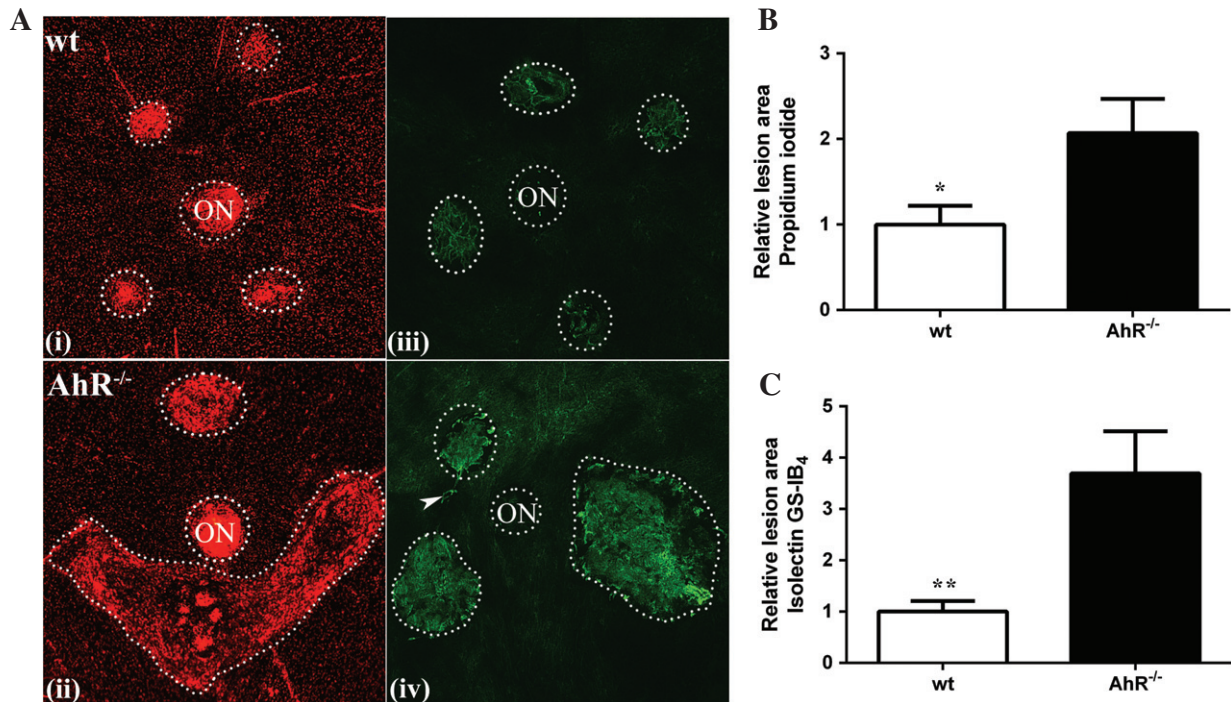
Figure 3. AhR regulates laser-induced CNV in young mice. (A) Choroidal flat-mounts were prepared from 4 month-old laser-induced CNV mice ($n = 8$/genotype) and stained with propidium iodide ($AhR^{-/-}$, AhR knock-out; ON, optic nerve; i, wt; ii, $AhR^{-/-}$) and isolectin GS-IB$_4$ (iii, wt; iv, $AhR^{-/-}$); arrowhead, vessels sprouting and extending out from the CNV lesion: representative images are shown (dotted circles demarcate lesions and ON). (B) Relative lesion area/animal measured in propidium iodide stained flat-mounts (mean and SEM; $n = 5$/group; $^*p < 0.05$). (C) Relative lesion area/animal measured in isolectin GS-IB$_4$-stained flat-mounts (mean and SEM; $n = 8$/group; $^{**}p < 0.01$)
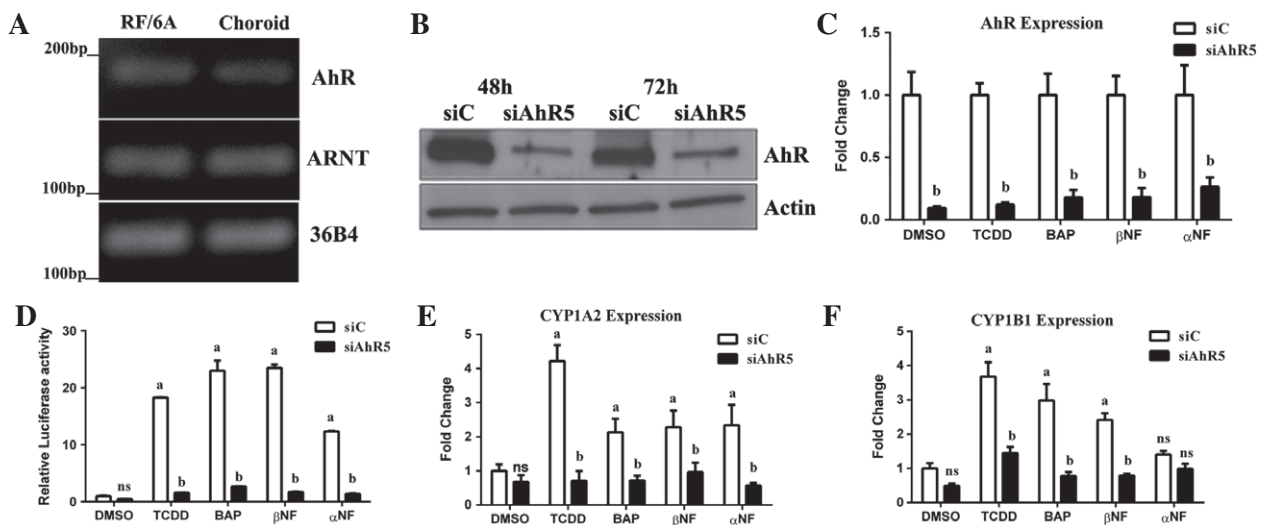

Figure 4. AhR pathway is active in choroidal RF/6A cells. (A) Agarose gel of PCR analysis of *AhR* and its obligate binding partner *ARNT* in RF/6A cells and human choroid tissue samples; 36B4 was used as loading control. (B) Western blot of *AhR* knock-down in RF/6A at 48 and 72 h (siC, control siRNA; siAhR5, *AhR* siRNA; $n = 3$, representative image shown); β-actin was used as loading control. (C) Expression of *AhR* in siC- and siAhR5-treated cells in response to known AhR agonists (TCDD, BAP, βNF) and a partial AhR agonist (αNF); DMSO was used as a control ($n = 3$). (D) AhR activity in RF/6A cells transfected with the AhR–tk–luciferase reporter and siC or siAhR; cells were treated with AhR agonists or DMSO as control ($n = 3$): a, $p < 0.05$ relative to DMSO-treated cells; b, $p < 0.05$ relative to drug–siC-treated cells ($p < 0.05$). (E) Expression of *CYP1A2* and (F) *CYP1B1* mRNA in siC- and siAhR-treated cells in response to AhR agonists or DMSO as a control ($n = 3$); a, $p < 0.05$ relative to DMSO-treated cells; b, $p < 0.05$ relative to drug-siC-treated cells; ns: not significant

in the laser-induced CNV lesions of $AhR^{-/-}$ versus wt mice. A marked increase in the quantity of COL4 staining within lesions in $AhR^{-/-}$ as compared to wt mice was noted (Figure 7A, B; $p < 0.001$). Furthermore, we confirmed that *AhR* knock-down leads to increased COL4 α4 (*COL4A4*) expression in, and secretion from,

ARPE19 as well as RF/6A cells (Figure 7C–F; *AhR* $p < 0.0001$, *COL4A4* $p < 0.001$). *AhR* knock-down also led to an increase in *COL1A1* expression in RF/6A cells (Figure 7D; *AhR* $p < 0.0001$, *COL1A1* $p < 0.001$) and a decrease in matrix metalloproteinase 2 (*MMP2*) expression in both ARPE19 (Figure 7C; $p < 0.0001$)
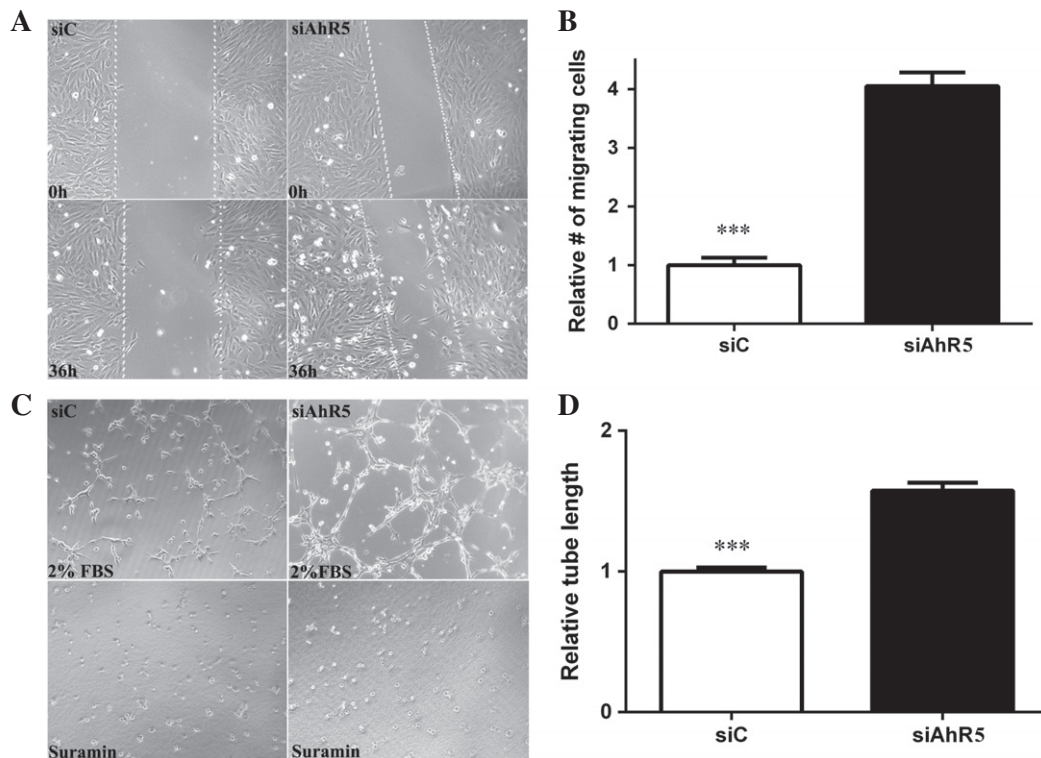
Figure 5. *AhR* knock-down increases endothelial migration and tube formation. (A) The effect of *AhR* loss on migration of RF/6A cells was analysed in a wound-healing assay ($n = 3$, representative images at $t = 0$ and $t = 36$ h are shown); dotted lines demarcate the boarders of the scrape wound. (B) The cells migrating into the wound were counted using ImageJ (mean and SEM; $n = 3$; $^*p < 0.0001$). (C) The effect of *AhR* loss on tube formation in RF/6A cells was analysed by an angiogenesis assay in Geltrex™ ($n = 3$; representative images at $t = 3$ h are shown). Suramin, an inhibitor of tube formation, was used as a negative control. (D) Quantification of tube length in Geltrex™ using ImageJ (mean and SEM; $n = 3$; $^*p < 0.0001$); siC, control siRNA; siAhR5, AhR siRNA

and RF/6A cells (Figure 7D; $p < 0.0001$). Finally, to distinguish between COL4 associated with vascular basement membrane versus the extracellular matrix of the CNV lesion, we examined the immunolocalization pattern of the blood vessel markers smooth muscle protein 22α (transgelin-TAGLN) and α-smooth muscle actin (ACTA2) within CNV lesions of *AhR*$^{-/-}$ and wt mice (see supplementary material, Figure S7). No genotype-specific differences in the staining pattern were seen, supporting the finding that increased COL4 is a not a consequence of an increase in the number of vessels and/or associated vascular basement membranes.

Discussion

AhR expression and activity not only sustains important cellular functions, such as cell proliferation, differentiation and migration, but also maintains vascular homeostasis and angiogenesis [55–60]. In this study, using *in vitro* and *in vivo* models in which *AhR* expression and activity was altered, we investigated the potential role of this receptor in the biology of wet AMD. We show that *AhR* regulates: (a) multiple pathways involved in the pathogenesis of wet AMD; and (b) the formation and severity of neovascular lesions in an animal model of CNV. Further, *AhR* knock-down increases the ability of endothelial cells to migrate and

form tube-like structures in a 3D matrix *in vitro*, an activity that results in an alteration of the RPE-choroid microenvironment. Taking into account the results from previous studies demonstrating that *AhR* activity decreases as a function of age [24–27], our findings support the hypothesis that targeting the AhR signalling pathway may be a viable approach to developing potential therapies to treat wet AMD patients.

The observation that *AhR* knock-out exacerbates CNV lesions in a murine model of wet AMD is novel, and verifies that the *AhR* plays an important role in maintaining both the RPE and the choroidal architecture and their responses to laser-induced injury. In some respects this is not surprising, as *AhR*-null mice develop increased ischaemia-induced angiogenesis compared to wt mice [61], as well as cardiac hypertrophy consequent to coronary neovascularization, concomitant with increased *VEGFA* and hypoxia-inducible factor 1α expression in the heart [62,63]. However, multiple studies have shown that *AhR*-null mice have hepatic vascular defects, impaired angiogenesis, decreased cell proliferation and migration that can compromise tumour xenograft growth [62,64–67]. This differential effect of *AhR*, resulting in pro- or anti-angiogenesis, may be cell type- and tissue-dependent [64]. In fact, in our cohort of *AhR*$^{-/-}$ mice, RNA expression and qPCR validation revealed a significant down-regulation of *Gpr124*, an orphan seven-pass transmembrane receptor,
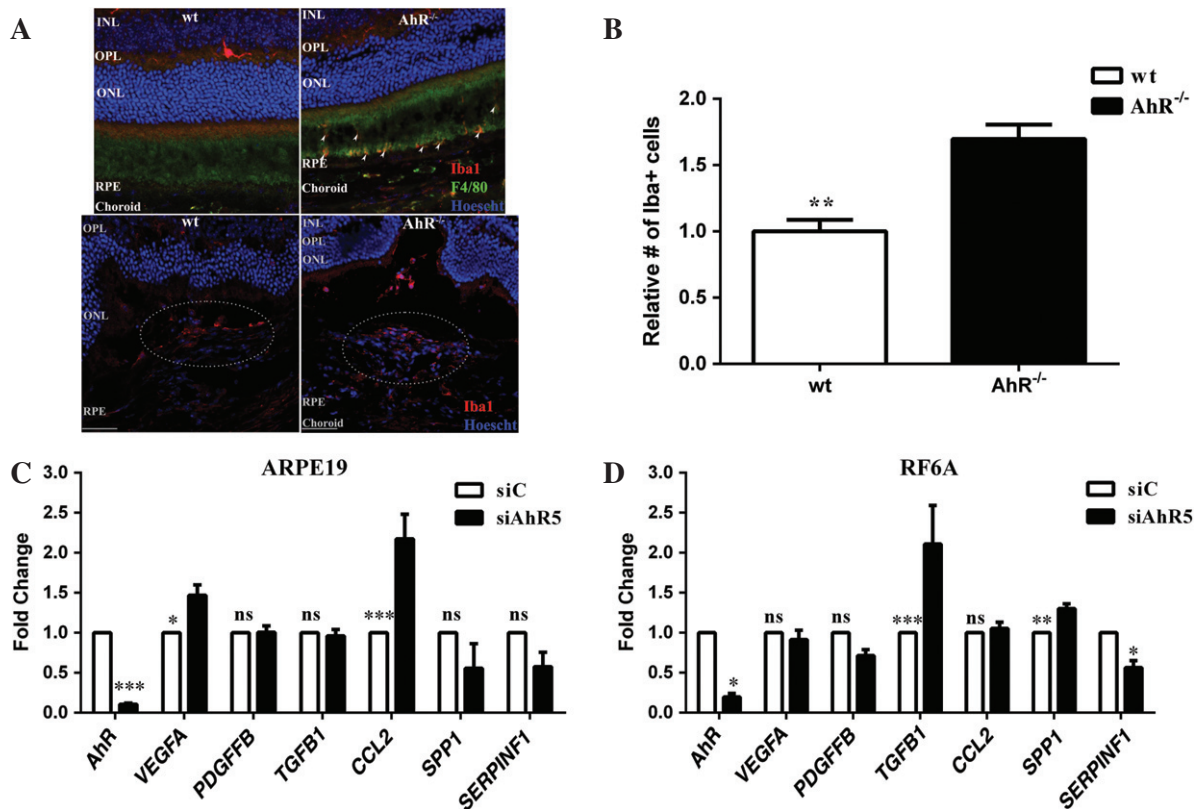
Figure 6. *AhR* regulates microglial infiltration and angiogenesis in CNV lesions. (A) Iba1 immunopositive cells (red) accumulate subretinally in 11–13 month-old *AhR*^{−/−} mice (top right) and within laser-induced CNV lesions of *AhR*^{−/−} mice (bottom right); Iba1^{+} cells are absent from the subretinal region in wt mice (top left) and decreased in wt CNV lesions (bottom left); dotted oval demarcates the lesion area in the bottom panels; nuclei are stained blue with Hoechst; representative images are shown; scale bar = 50 µm. (B) The numbers of Iba1^{+} cells in the CNV lesions of wt and *AhR*^{−/−} mice were counted using ImageJ (mean and SEM; $n = 4$/group; [*]$p < 0.001$). (C, D) Effect of *AhR* loss on *VEGFA*, *PDGFFB*, *TGFB1*, *CCL2*, *SPP1* and *SERPINF1* mRNA expression, using qPCR in (C) ARPE19 cells (mean and SEM; $n = 3$; [*]$p < 0.01$, [***]$p < 0.0001$) and (D) RF/6A cells (mean and SEM; $n = 3$; [*]$p < 0.05$, [**]$p < 0.001$, [***]$p < 0.0001$); siC, control siRNA; siAhR5, AhR siRNA; INL, inner nuclear layer; OPL, outer plexiform layer; ONL, outer nuclear layer; ns, not significant

which has been shown to up-regulate *VEGFA* expression [36]. The severity of the neovascular lesions can be further explained by examining both the effect of *AhR* knock-down on RPE and choroidal endothelial cell phenotypes, as well as increased expression of pro-angiogenic factors. We found that *AhR* knock-down in ARPE19 cells did not affect cell migration (data not shown) but resulted in an increase in *VEGFA* expression. In contrast, RF/6A endothelial cells responded to *AhR* knock-down by an increase in their ability to migrate and morph into tube-like structures when plated in a 3D matrix.

Another AMD-relevant pro-angiogenic modulator is *CCL2*. This angiogenic chemokine is a critical regulator of migration of monocytes and macrophages and has also been shown to mediate *TGFβ*-induced angiogenesis [68]. In the eye, it has been reported to be up-regulated in aged mouse retinas [41,42], in RPE in AMD eyes [69] and in the aqueous humor of CNV patients [70]. The larger lesions observed in our cohort of *AhR*^{−/−} mice could be due in part to an increased number of Iba1^{+} microglial cells localized within the lesion subsequent to up-regulation of *CCL2* in ARPE19 cells, in concert with increased *SPP1* and *TGFB1* expression in RF/6A cells. Collectively, these observations support the

postulate that AhR dysfunction exacerbates an already pro-angiogenic environment. Our findings may appear to contradict studies that have shown that AhR agonists also stimulate *CCL2* expression in human umbilical cord vein endothelial cells [71,72]. However, this is not surprising, considering the vital role of the AhR in clearance and the fundamental phagocytic responsibility of macrophages. The inflammatory status of the macrophages recruited within the lesions, critical to their overall function [73,74], remains to be determined.

A role for AhR in ECM remodelling has already been established; *AhR* knock-out mice develop liver fibrosis concomitant with an increase in *TGFB1* and collagen expression [75,76]. Consistent with these reports, we also observed increased production and deposition of the ECM molecule COL4. Specifically, *AhR*^{−/−} mice displayed greater COL4 deposition in the CNV lesions compared to wt mice. In addition, we measured increased COL4 synthesis and secretion in both ARPE19 and RF/6A cells following *AhR* knock-down, supporting the role of the AhR signalling pathway in mediating matrix metabolism and deposition. ECM molecules, including COL4, are of great importance in the pathobiology of AMD, as they are abundant not only within sub-RPE deposits, which increase the risk for
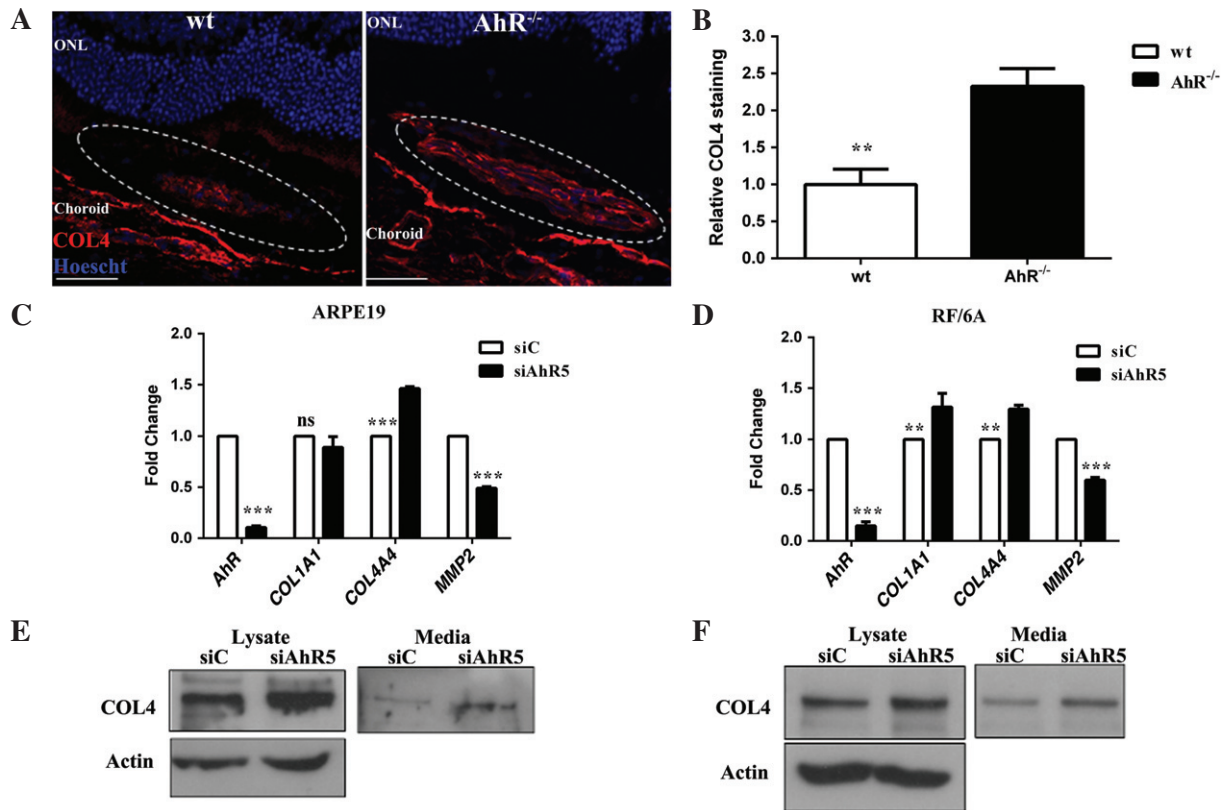
Figure 7. *AhR* regulates ECM deposition, production and secretion. (A) COL4 immunolocalization (red) in CNV lesions of wt and *AhR*$^{-/-}$ mice: dotted oval demarcates the lesion area; nuclei are stained blue with Hoechst; representative images are shown; scale bar = 50 µm. (B) COL4 staining intensity was quantified in the CNV lesions of wt and *AhR*$^{-/-}$ mice using ImageJ (mean and SEM; $n = 4$/group; $^{**}p < 0.001$). (C, D) Effect of *AhR* knock-down on *COL1A1*, *COL4A4* and *MMP2* mRNA expression in (C) ARPE19 cells and (D) RF/6A cells (mean and SEM; $n = 3$; $^{**}p < 0.001$, $^{***}p < 0.0001$; ns, not significant). (E, F) Effect of *AhR* loss on COL4 protein levels, as evaluated by western blot in (E) ARPE19 and (F) RF/6A cell lysates and secreted media ($n = 3$): representative images are shown; ONL, outer nuclear layer; siC, control siRNA; siAhR5, AhR siRNA

progression to wet AMD, but also within excised CNV membranes themselves [77]. Although the precise link between collagen and CNV formation is not known, it has been shown in the context of vascular biology to modulate angiogenesis, promoting vascular elongation, proliferation, stabilization and survival [78,79]. Another ECM regulatory molecule important in AMD is MMP2, whose activity is reportedly disrupted in Bruch's membrane isolated from human AMD donor eyes [80]. We observed a down-regulation of *MMP2* expression in ARPE19 and RF/6A cells with *AhR* knock-down. It should be noted that, although a decrease in COL1A1 expression was detected in our RNA-seq data, we were not able to confirm this expression change in the RPE and endothelial cell culture lines. This may not be surprising, given that we are comparing results obtained from expression studies on a complex multicellular tissue (RPE-choroid) harvested from an aged mouse to those from individual RPE or endothelial cell culture lines. Overall, our findings strengthen the hypothesis that *AhR*-mediated regulation of MMPs may contribute to impaired matrix degradation of Bruch's membrane and ultimately exacerbate pathology associated with AMD.

In summary, we found that decreased expression and activity of the *AhR* exacerbates murine neovascular AMD and increases cell migration and tube formation. The mechanism involves multiple AMD-related pathogenic pathways, including increased expression of pro-angiogenic mediators and altered matrix degradation. Our results suggest that the *AhR* may be important in the regulation of pathways of pathological importance in AMD. Future studies will focus on investigating the therapeutic benefits of targeting the *AhR* signalling pathway as a means of treating angiogenesis and fibrosis in wet AMD.

Acknowledgements

Author contributions

MC, PH and GM designed and performed research; DK, RT and DPM contributed new reagents/analytic tools; MC, DK and GM analysed data; and MC and GM wrote the paper.

Abbreviations

AhR, aryl hydrocarbon receptor; AMD, age-related macular degeneration; ANOVA, analysis of variance; ARVO, Association of Research in Vision and Ophthalmology; BCA, bicinchoninic acid; bHLH/PAS, basic helix−loop−helix/Per−Arnt−Sim; CCL2, chemokine (C−C motif) ligand 2; CNV, choroidal neovascularization; COL, collagen; CYP1A2, cytochrome P450, family 1, subfamily A, polypeptide 2; CYP1B1, cytochrome P450, family 1, subfamily B, polypeptide 1; ECM, extracellular matrix; EDTA, ethylenediaminetetra-acetic acid; FPKM, fragments/kilobase of exon/million fragments mapped; GO, Gene Ontology; Iba1, ionized calcium-binding adaptor molecule 1; MMP, matrix metalloproteinase; PCR, polymerase chain reaction; RNA-seq, RNA sequencing; RPE, retinal pigment epithelium; SDS−PAGE, sodium dodecyl sulphate−polyacrylamide gel electrophoresis; siRNA, small interfering RNA; TCDD, tetrachlorodibenzodioxin; TGFB1, transforming growth factor-β1; VEGFA, vascular endothelial growth factor A; wt, wild-type.

References

1. Jager RD, Mieler WF, Miller JW. Age-related macular degeneration. *N Engl J Med* 2008; **358:** 2606−2617.
2. Friedman DS, O'Colmain BJ, Munoz B, *et al.* Prevalence of age-related macular degeneration in the United States. *Arch Ophthalmol* 2004; **122:** 564−572.
3. Chen Y, Bedell M, Zhang K. Age-related macular degeneration: genetic and environmental factors of disease. *Mol Interv* 2010; **10:** 271−281.
4. Ambati J, Fowler BJ. Mechanisms of age-related macular degeneration. *Neuron* 2012; **75:** 26−39.
5. Schlingemann RO. Role of growth factors and the wound healing response in age-related macular degeneration. *Graefes Arch Clin Exp Ophthalmol* 2004; **242:** 91−101.
6. Dahlmann AH, Mireskandari K, Cambrey AD, *et al.* Current and future prospects for the prevention of ocular fibrosis. *Ophthalmol Clin N Am* 2005; **18:** 539−559.
7. Kent D, Sheridan C. Choroidal neovascularization: a wound healing perspective. *Mol Vis* 2003; **9:** 747−755.
8. Bloch SB, Lund-Andersen H, Sander B, *et al.* Subfoveal fibrosis in eyes with neovascular age-related macular degeneration treated with intravitreal ranibizumab. *Am J Ophthalmol* 2013; **156:** 116−124 e111.
9. Baird PN, Robman LD, Richardson AJ, *et al.* Gene−environment interaction in progression of AMD: the *CFH* gene, smoking and exposure to chronic infection. *Hum Mol Genet* 2008; **17:** 1299−1305.
10. Donoso LA, Vrabec T, Kuivaniemi H. The role of complement Factor H in age-related macular degeneration: a review. *Surv Ophthalmol* 2010; **55:** 227−246.
11. Tomany SC, Wang JJ, Van Leeuwen R, *et al.* Risk factors for incident age-related macular degeneration: pooled findings from three continents. *Ophthalmology* 2004; **111:** 1280−1287.
12. Booij JC, ten Brink JB, Swagemakers SM, *et al.* A new strategy to identify and annotate human RPE-specific gene expression. *PLoS One* 2010; **5:** e9341.
13. Newman AM, Gallo NB, Hancox LS, *et al.* Systems-level analysis of age-related macular degeneration reveals global biomarkers and phenotype-specific functional networks. *Genome Med* 2012; **4:** 16.
14. Denison MS, Nagy SR. Activation of the aryl hydrocarbon receptor by structurally diverse exogenous and endogenous chemicals. *Annu Rev Pharmacol Toxicol* 2003; **43:** 309−334.
15. Barouki R, Coumoul X, Fernandez-Salguero PM. The aryl hydrocarbon receptor, more than a xenobiotic-interacting protein. *FEBS Lett* 2007; **581:** 3608−3615.
16. Phillips DH. Polycyclic aromatic hydrocarbons in the diet. *Mutat Res* 1999; **443:** 139−147.
17. Pryor WA. Cigarette smoke radicals and the role of free radicals in chemical carcinogenicity. *Environ Health Perspect* 1997; **105**(suppl 4): 875−882.
18. Gomez-Duran A, Carvajal-Gonzalez JM, Mulero-Navarro S, *et al.* Fitting a xenobiotic receptor into cell homeostasis: how the dioxin receptor interacts with TGFbeta signaling. *Biochem Pharmacol* 2009; **77:** 700−712.
19. Ishimura R, Kawakami T, Ohsako S, et al. Dioxin-induced toxicity on vascular remodeling of the placenta. *Biochem Pharmacol* 2009; **77:** 660−669.
20. Dietrich C, Kaina B. The aryl hydrocarbon receptor (AhR) in the regulation of cell−cell contact and tumor growth. *Carcinogenesis* 2010; **31:** 1319−1328.
21. Tsay JJ, Tchou-Wong KM, Greenberg AK, *et al.* Aryl hydrocarbon receptor and lung cancer. *Anticancer Res* 2013; **33:** 1247−1256.
22. Wu D, Nishimura N, Kuo V, *et al.* Activation of aryl hydrocarbon receptor induces vascular inflammation and promotes atherosclerosis in apolipoprotein E$^{-/-}$ mice. *Arterioscler Thromb Vasc Biol* 2011; **31:** 1260−1267.
23. Ichihara S. The pathological roles of environmental and redox stresses in cardiovascular diseases. *Environ Health Prev Med* 2013; **18:** 177−184.
24. Hu P, Herrmann R, Bednar A, *et al.* Aryl hydrocarbon receptor deficiency causes dysregulated cellular matrix metabolism and age-related macular degeneration-like pathology. *Proc Natl Acad Sci USA* 2013; **110:** E4069−4078.
25. Carlstedt-Duke JM. Tissue distribution of the receptor for 2,3,7,8-tetrachlorodibenzo-*p*-dioxin in the rat. *Cancer Res* 1979; **39:** 3172−3176.
26. Kahl GF, Friederici DE, Bigelow SW, *et al.* Ontogenetic expression of regulatory and structural gene products associated with the Ah locus. Comparison of rat, mouse, rabbit and *Sigmoden hispedis*. *Dev Pharmacol Ther* 1980; **1:** 137−162.
27. Sommer RJ, Sojka KM, Pollenz RS, *et al.* Ah receptor and ARNT protein and mRNA concentrations in rat prostate: effects of stage of development and 2,3,7,8-tetrachlorodibenzo-*p*-dioxin treatment. *Toxicol Appl Pharmacol* 1999; **155:** 177−189.
28. Lahvis GP, Bradfield CA. *Ahr*-null alleles: distinctive or different? *Biochem Pharmacol* 1998; **56:** 781−787.
29. Tariq MA, Kim HJ, Jejelowo O, *et al.* Whole-transcriptome RNAseq analysis from minute amount of total RNA. *Nucleic Acids Res* 2011; **39:** e120.
30. Wang Z, Gerstein M, Snyder M. RNA-Seq: a revolutionary tool for transcriptomics. *Nat Rev Genet* 2009; **10:** 57−63.

31. Anders S, Pyl PT, Huber W. HTSeq – a Python framework to work with high-throughput sequencing data. *bioRxiv* 2014: 1–6.

32. Robinson MD, McCarthy DJ, Smyth GK. edgeR: a Bioconductor package for differential expression analysis of digital gene expression data. *Bioinformatics* 2010; **26:** 139–140.

33. Robinson MD, Smyth GK. Moderated statistical tests for assessing differences in tag abundance. *Bioinformatics* 2007; **23:** 2881–2887.

34. Espinosa-Heidmann DG, Malek G, Mettu PS, *et al.* Bone marrow transplantation transfers age-related susceptibility to neovascular remodeling in murine laser-induced choroidal neovascularization. *Invest Ophthalmol Vis Sci* 2013; **54:** 7439–7449.

35. Wang Y, Cho SG, Wu X, *et al.* G-protein coupled receptor 124 (GPR124) in endothelial cells regulates vascular endothelial growth factor (VEGF)-induced tumor angiogenesis. *Curr Mol Med* 2014; **14:** 543–554.

36. Cullen M, Elzarrad MK, Seaman S, *et al.* GPR124, an orphan G protein-coupled receptor, is required for CNS-specific vascularization and establishment of the blood–brain barrier. *Proc Natl Acad Sci USA* 2011; **108:** 5759–5764.

37. Grunin M, Burstyn-Cohen T, Hagbi-Levi S, *et al.* Chemokine receptor expression in peripheral blood monocytes from patients with neovascular age-related macular degeneration. *Invest Ophthalmol Vis Sci* 2012; **53:** 5292–5300.

38. Grunin M, Hagbi-Levi S, Chowers I. The role of monocytes and macrophages in age-related macular degeneration. *Adv Exp Med Biol* 2014; **801:** 199–205.

39. Nigro J, Dilley RJ, Little PJ. Differential effects of gemfibrozil on migration, proliferation and proteoglycan production in human vascular smooth muscle cells. *Atherosclerosis* 2002; **162:** 119–129.

40. Gupta N, Brown KE, Milam AH. Activated microglia in human retinitis pigmentosa, late-onset retinal degeneration, and age-related macular degeneration. *Exp Eye Res* 2003; **76:** 463–471.

41. Xu H, Chen M, Forrester JV. Para-inflammation in the aging retina. *Prog Retin Eye Res* 2009; **28:** 348–368.

42. Xu H, Chen M, Manivannan A, *et al.* Age-dependent accumulation of lipofuscin in perivascular and subretinal microglia in experimental mice. *Aging Cell* 2008; **7:** 58–68.

43. Streilein JW, Ma N, Wenkel H, *et al.* Immunobiology and privilege of neuronal retina and pigment epithelium transplants. *Vision Res* 2002; **42:** 487–495.

44. Shi G, Maminishkis A, Banzon T, *et al.* Control of chemokine gradients by the retinal pigment epithelium. *Invest Ophthalmol Vis Sci* 2008; **49:** 4620–4630.

45. Ng TF, Streilein JW. Light-induced migration of retinal microglia into the subretinal space. *Invest Ophthalmol Vis Sci* 2001; **42:** 3301–3310.

46. Huang H, Parlier R, Shen JK, *et al.* VEGF Receptor blockade markedly reduces retinal microglia/macrophage infiltration into laser-induced CNV. *PLoS One* 2013; **8:** e71808.

47. Zhang H, Liu ZL. Transforming growth factor-β neutralizing antibodies inhibit subretinal fibrosis in a mouse model. *Int J Ophthalmol* 2012; **5:** 307–311.

48. Kiefer MC, Bauer DM, Barr PJ. The cDNA and derived amino acid sequence for human osteopontin. *Nucleic Acids Res* 1989; **17:** 3306.

49. Wang KX, Denhardt DT. Osteopontin: role in immune regulation and stress responses. *Cytokine Growth Factor Rev* 2008; **19:** 333–345.

50. Zarbin MA. Current concepts in the pathogenesis of age-related macular degeneration. *Arch Ophthalmol* 2004; **122:** 598–614.

51. Reale E, Groos S, Eckardt U, *et al.* New components of 'basal laminar deposits' in age-related macular degeneration. *Cells Tissues Organs* 2009; **190:** 170–181.

52. Grossniklaus HE, Martinez JA, Brown VB, *et al.* Immunohistochemical and histochemical properties of surgically excised subretinal neovascular membranes in age-related macular degeneration. *Am J Ophthalmol* 1992; **114:** 464–472.

53. Kung T, Murphy KA, White LA. The aryl hydrocarbon receptor (AhR) pathway as a regulatory pathway for cell adhesion and matrix metabolism. *Biochem Pharmacol* 2009; **77:** 536–546.

54. Aragon AC, Kopf PG, Campen MJ, *et al.* In utero and lactational 2,3,7,8-tetrachlorodibenzo-*p*-dioxin exposure: effects on fetal and adult cardiac gene expression and adult cardiac and renal morphology. *Toxicol Sci* 2008; **101:** 321–330.

55. Wang K, Li Y, Jiang YZ, *et al.* An endogenous aryl hydrocarbon receptor ligand inhibits proliferation and migration of human ovarian cancer cells. *Cancer Lett* 2013; **340:** 63–71.

56. Barouki R, Aggerbeck M, Aggerbeck L, *et al.* The aryl hydrocarbon receptor system. *Drug Metabol Drug Interact* 2012; **27:** 3–8.

57. De Abrew KN, Kaminski NE, Thomas RS. An integrated genomic analysis of aryl hydrocarbon receptor-mediated inhibition of B-cell differentiation. *Toxicol Sci* 2010; **118:** 454–469.

58. Tanos R, Murray IA, Smith PB, *et al.* Role of the Ah receptor in homeostatic control of fatty acid synthesis in the liver. *Toxicol Sci* 2012; **129:** 372–379.

59. Olufsen M, Arukwe A. Developmental effects related to angiogenesis and osteogenic differentiation in salmon larvae continuously exposed to dioxin-like 3,3′,4,4′-tetrachlorobiphenyl (congener 77). *Aquat Toxicol* 2011; **105:** 669–680.

60. Hall JM, Barhoover MA, Kazmin D, *et al.* Activation of the aryl-hydrocarbon receptor inhibits invasive and metastatic features of human breast cancer cells and promotes breast cancer cell differentiation. *Mol Endocrinol* 2010; **24:** 359–369.

61. Ichihara S, Yamada Y, Ichihara G, *et al.* A role for the aryl hydrocarbon receptor in regulation of ischemia-induced angiogenesis. *Arterioscler Thromb Vasc Biol* 2007; **27:** 1297–1304.

62. Fernandez-Salguero PM, Ward JM, Sundberg JP, *et al.* Lesions of aryl-hydrocarbon receptor-deficient mice. *Vet Pathol* 1997; **34:** 605–614.

63. Thackaberry EA, Gabaldon DM, Walker MK, *et al.* Aryl hydrocarbon receptor-null mice develop cardiac hypertrophy and increased hypoxia-inducible factor-1α in the absence of cardiac hypoxia. *Cardiovasc Toxicol* 2002; **2:** 263–274.

64. Contador-Troca M, Alvarez-Barrientos A, Barrasa E, *et al.* The dioxin receptor has tumor suppressor activity in melanoma growth and metastasis. *Carcinogenesis* 2013; **34:** 2683–2693.

65. Fernandez-Salguero P, Pineau T, Hilbert DM, *et al.* Immune system impairment and hepatic fibrosis in mice lacking the dioxin-binding Ah receptor. *Science* 1995; **268:** 722–726.

66. Mulero-Navarro S, Pozo-Guisado E, Perez-Mancera PA, *et al.* Immortalized mouse mammary fibroblasts lacking dioxin receptor have impaired tumorigenicity in a subcutaneous mouse xenograft model. *J Biol Chem* 2005; **280:** 28731–28741.

67. Fritz WA, Lin TM, Peterson RE. The aryl hydrocarbon receptor (AhR) inhibits vanadate-induced vascular endothelial growth factor (VEGF) production in TRAMP prostates. *Carcinogenesis* 2008; **29:** 1077–1082.

68. Ma J, Wang Q, Fei T, *et al.* MCP-1 mediates TGF-β-induced angiogenesis by stimulating vascular smooth muscle cell migration. *Blood* 2007; **109:** 987–994.

69. Grossniklaus HE, Ling JX, Wallace TM, *et al.* Macrophage and retinal pigment epithelium expression of angiogenic cytokines in choroidal neovascularization. *Mol Vis* 2002; **8:** 119–126.

70. Jonas JB, Tao Y, Neumaier M, *et al.* Monocyte chemoattractant protein 1, intercellular adhesion molecule 1, and vascular cell adhesion molecule 1 in exudative age-related macular degeneration. *Arch Ophthalmol* 2010; **128:** 1281–1286.

71. Knaapen AM, Curfs DM, Pachen DM, *et al.* The environmental carcinogen benzo[a]pyrene induces expression of monocyte-chemoattractant protein-1 in vascular tissue: a possible role in atherogenesis. *Mutat Res* 2007; **621:** 31–41.

72. Watanabe I, Tatebe J, Namba S, *et al.* Activation of aryl hydrocarbon receptor mediates indoxyl sulfate-induced monocyte chemoattractant protein-1 expression in human umbilical vein endothelial cells. *Circ J* 2013; **77:** 224–230.

73. Kigerl KA, Gensel JC, Ankeny DP, *et al.* Identification of two distinct macrophage subsets with divergent effects causing either neurotoxicity or regeneration in the injured mouse spinal cord. *J Neurosci* 2009; **29:** 13435–13444.

74. Barros MH, Hauck F, Dreyer JH, *et al.* Macrophage polarization: an immunohistochemical approach for identifying M1 and M2 macrophages. *PLoS One* 2013; **8:** e80908.

75. Zaher H, Fernandez-Salguero PM, Letterio J, *et al.* The involvement of aryl hydrocarbon receptor in the activation of transforming growth factor-β and apoptosis. *Mol Pharmacol* 1998; **54:** 313–321.

76. Carvajal-Gonzalez JM, Roman AC, Cerezo-Guisado MI, *et al.* Loss of dioxin-receptor expression accelerates wound healing *in vivo* by a mechanism involving TGFβ. *J Cell Sci* 2009; **122:** 1823–1833.

77. Grossniklaus HE, Miskala PH, Green WR, *et al.* Histopathologic and ultrastructural features of surgically excised subfoveal choroidal neovascular lesions: submacular surgery trials report no. 7. *Arch Ophthalmol* 2005; **123:** 914–921.

78. Bonanno E, Iurlaro M, Madri JA, *et al.* Type IV collagen modulates angiogenesis and neovessel survival in the rat aorta model. *In Vitro Cell Dev Biol Anim* 2000; **36:** 336–340.

79. Cao J, Zhao L, Li Y, *et al.* A subretinal matrigel rat choroidal neovascularization (CNV) model and inhibition of CNV and associated inflammation and fibrosis by VEGF trap. *Invest Ophthalmol Vis Sci* 2010; **51:** 6009–6017.

80. Hussain AA, Lee Y, Zhang JJ, *et al.* Disturbed matrix metalloproteinase activity of Bruch's membrane in age-related macular degeneration. *Invest Ophthalmol Vis Sci* 2011; **52:** 4459–4466.

SUPPLEMENTARY MATERIAL ON THE INTERNET

The following supplementary material may be found in the online version of this article:

Supplementary materials and methods

Figure S1. Fetal bovine serum does not contribute to secreted protein expression

Figure S2. Enlarged 3D reconstruction images of the thickness of laser-induced CNV lesions in wt and $AhR^{-/-}$ mice

Figure S3. Validation of *AhR* knock-down using different siRNA sequences

Figure S4. *AhR* knock-down does not affect cell viability and proliferation

Figure S5. *AhR* knock-down does not lead to secretion of pro-proliferative stimuli within the medium

Figure S6. CNV lesions in $AhR^{-/-}$ mouse eyes display an increased number of SPP1-positive cells

Figure S7. CNV lesions in wt and $AhR^{-/-}$ mouse eyes display no difference in vessel staining

Table S1. Human primers and siRNA sequences

Table S2. Antibodies, sources and applications

Table S3. Mouse primer sequences

Table S4. List of drugs, concentrations, and sources

Table S5. List of differentially expressed genes and their GO classifications

25 Years ago in the *Journal of Pathology…*

Type VII collagen antibody LH 7.2 identifies basement membrane characteristics of thin malignant melanomas

Dr Nigel Kirkham, Margaret L. Price, Barry Gibson, Irene M. Leigh, Peter Coburn and Charles R. Darley

To view these articles, and more, please visit: www.thejournalofpathology.com

Click 'ALL ISSUES (1892 - 2011)', to read articles going right back to Volume 1, Issue 1.

The Journal of Pathology
Understanding Disease

Journal of
The Pathological Society